[26]A. A. Maradudin (private communication).
[27]E. W. Kellermann, Phil. Trans. Roy. Soc. London 238, 513 (1940).
[28]See Ref. 24.
[29]A listing of the ionic displacements and the dipole moments can be obtained from the authors upon request.

PHYSICAL REVIEW B VOLUME 5, NUMBER 8 15 APRIL 1972

Optical and EPR Studies of $[Na]^0$ and $[Li]^0$ Centers in CaO†

H. T. Tohver, * B. Henderson,‡ Y. Chen, and M. M. Abraham
Solid State Division, Oak Ridge National Laboratory, Oak Ridge, Tennessee 37830
(Received 12 October 1971)

We report EPR and optical studies of O^- ions located next to Li^+ and Na^+ impurities in calcium oxide. The oscillator strengths of the optical transitions ($f \sim 0.1$) are larger than expected for the $A(p_z) \rightarrow E(p_x, p_y)$ transitions of these centers. The hyperfine interaction with the impurity nuclei is interpreted as having a negative contact term a and a positive anisotropic term b. The results are discussed in terms of admixture of $O^-|3s\rangle$ functions into the ground p_z state.

I. INTRODUCTION

The optical absorption bands of trapped electron and trapped hole centers in the alkali halides were studied long before models for the defects were accepted and before EPR and electron-nuclear double resonance (ENDOR) techniques were available to guide the choice of model. For the alkaline-earth oxides, the order of study was reversed and the EPR spectra of F^+ and V^- centers were identified first.[1] Presently the F^+ bands are reasonably well understood (albeit only after some controversy), but less attention has been given to the optical properties of trapped hole centers.

Trapped hole centers have very different structures in the isostructural alkali halides and alkaline-earth oxides. In the alkali halides, the intrinsic hole centers are the self-trapped X_2^- molecule ions, whose symmetry axes are parallel to the crystal ⟨110⟩ directions.[2] Although mixed molecule ions, $(OF)^{2-}$, have been observed in magnesium oxide crystals containing fluorine,[3] no EPR spectrum has been identified which can be attributed to O_2^{3-}, the analog of the X_2^- center in any of the alkaline-earth oxides. Instead, crystals of the alkaline-earth oxides irradiated with x rays, γ rays, or fast electrons show magnetic resonance absorption due to V^- centers, i.e., O^- ions adjacent to cation vacancies.[1] It can be seen in Fig. 1 that the V^- centers have tetragonal symmetry about the principal axes of the crystal.

The presence of trapped hole centers in MgO crystals subjected to ionizing radiation was first detected with EPR methods by Wertz *et al.*[1] These authors observed a three-line spectrum at arbitrary orientations with turning points about the ⟨100⟩ crystal direction. Analysis of the spectrum showed the g tensor to have cylindrical symmetry around the ⟨100⟩ axes with $g_\perp = 2.0385$ and $g_\parallel = 2.0033$. No central ion hyperfine pattern was reported. It was proposed that the spectrum was associated with the V^- center, an O^- ion adjacent to a cation vacancy. This proposed model was based upon the g values, saturation properties, and temperature dependence of the spectrum. Strong support came later from EPR and ENDOR measurements of the interactions between the trapped hole and neighboring OH^-, OD^-, or F^- impurities.[4] More recently, hyperfine interaction with the adjacent Mg^{2+} ions, of which only the 10% abundant ^{25}Mg nuclides are magnetic, has been observed.[5] Similarly, simple EPR spectra have now been observed for V^- centers in CaO[6] and SrO.[7,8] In all three oxides, the measured values of $g_\perp$ were significantly greater than the g value for free electrons. EPR spectra of O^- ions adjacent to substitutional Li^+ ions ($[Li]^0$ centers) in MgO, CaO, and SrO have also been reported.[9] A schematic representation of the structure of these and related defects in the alkaline-earth oxides is portrayed in Fig. 1. In the present paper, detailed optical and EPR resonance measurements on the $[Li]^0$ and $[Na]^0$ centers in CaO are discussed.

II. EXPERIMENTAL

Single crystals of CaO were grown from Mallinckrodt $CaCO_3$ powder, reagent grade, by submerged arc fusion.[10] The starting powder contained about 10% by weight of Na_2CO_3 or Li_2CO_3. An analysis of the resulting crystals showed there to be approximately 1300 ppm of Li or 70 ppm of Na present after melting. All crystals were annealed to 1100 °C and then quenched to room temperature. For EPR studies, trapped hole centers were produced by irradiation at 10 K with 2-MeV

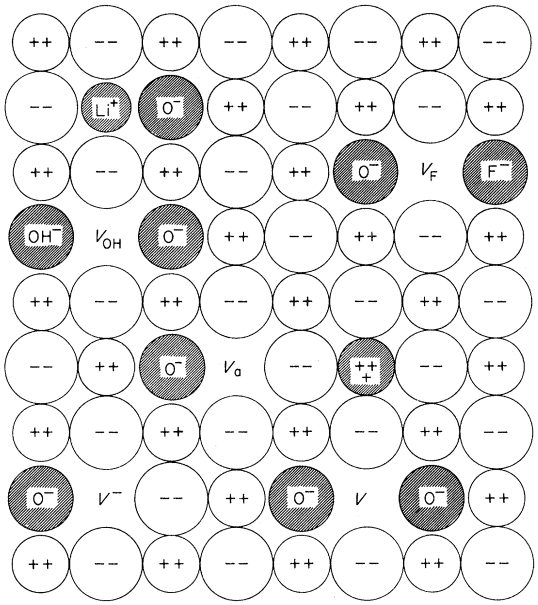

FIG. 1. Schematic representations of the structure of $[Li]^0$, V_{OH}, V^-, V, V_a, and V_F in alkaline-earth oxides.

electrons from a Van de Graaff accelerator at low current densities. A cryotip refrigerator with a suprasil cold finger which fitted directly into the sample access of the resonant cavity was used. Alternatively, crystals were irradiated at 77 K and then transferred to the EPR cavity with little intervening warmup ($\Delta T < 5$ K).

EPR measurements were made at 3-cm wavelength. In the temperature range 10–300 K we used a homodyne spectrometer employing a Varian V-4531 rectangular cavity and 100-kHz field modulation. Variable temperature was achieved using the cryotip heater and/or varying the helium flow in the cryotip. Measurements were also made at 1.5 K using a superheterodyne spectrometer with the klystron stabilized to an external cavity. Accurate measurements of the position of each hyperfine component were made using a proton magnetic resonance probe. The absence of drift in the frequency of the signal klystron over the period of the hyperfine measurements was ascertained by measuring with a direct reading microwave frequency counter at the beginning and end of each sequence of hyperfine lines.

In order to study the optical absorption of irradiated CaO crystals, cleaved plates of 1–7-mm thickness were mounted in a cryostat with optical windows. For irradiations and measurements at 77 K, a Sulfrian cryostat was used in conjunction with the Van de Graaff electron accelerator. Where comparative optical and EPR measurements were made, a common sample was used.

Isochronal annealing studies were carried out *in situ* in the optical cryostat or the EPR spectrometer. In both cases, the procedure was to start measurements at 77 K. The samples were then quickly warmed to some higher temperature between 77–300 K and held at that temperature for a period of 7 min. Subsequently the crystals were rapidly cooled to 77 K and the defect concentrations remeasured. For EPR measurements of the defect concentrations, a phosphorus-doped silicon standard was used.

III. EXPERIMENTAL RESULTS

A. EPR Spectra of $[Na]^0$ and $[Li]^0$ Centers

Following electron irradiation of the Na-doped crystals, EPR observations at 4 K showed a spectrum consisting of groups of four hyperfine components (Fig. 2). With $\vec{H}$ in the (100) plane, three such groups were observed, one of which remained invariant under rotations. The other two groups alternately varied in position between a minimum and a maximum field position for $\vec{H}$ along the [001] and [010] directions. Consequently, the defect has axial symmetry with a fourfold axis being parallel to one of the crystal [100] axes. The V^- center also has this symmetry. The hyperfine structure demonstrates the involvement of ^{23}Na ($I = \frac{3}{2}$), which is almost 100% abundant. We attributed the spectrum to the $[Na]^0$ center, an O^- ion adjacent to a Na^+ ion.

With the magnetic field parallel or perpendicular to a crystal ⟨100⟩ direction, only four hyperfine components ($\Delta m_I = 0$) are observed. From accurate measurements of the field positions in these orientations, it is evident that $A_\parallel < A_\perp$. At no orientation in the (100) plane does the hyperfine structure collapse and consequently $A_\parallel$ and $A_\perp$ must be of the same sign (i.e., A changes monotonically from $A_\parallel$ to $A_\perp$ and therefore cannot equal zero at some angle in the plane). It is not possible to determine the absolute sign of the hyperfine parameters. At orientations between $\theta = 0°$ and 90°, the hyperfine structure becomes complex. As shown in Fig. 2, this complexity is due to additional lines which appear between the main lines and which at some orientations rival the allowed transitions in intensity.

Below 10 K the $[Na]^0$ spectrum is easily saturated by microwave power. In this temperature range measurements with the homodyne spectrometer were confined to the minimum power level (40-dB attenuation of the available 300-mW klystron power). At this power level the intensity of the spectrum decreased with increasing temperature and could not be observed at 35 K. Increasing the microwave power then restored the spectrum to its former intensity. With further increase in temperature the lines were observed to broaden dramatically above 54 K such that a single broad line

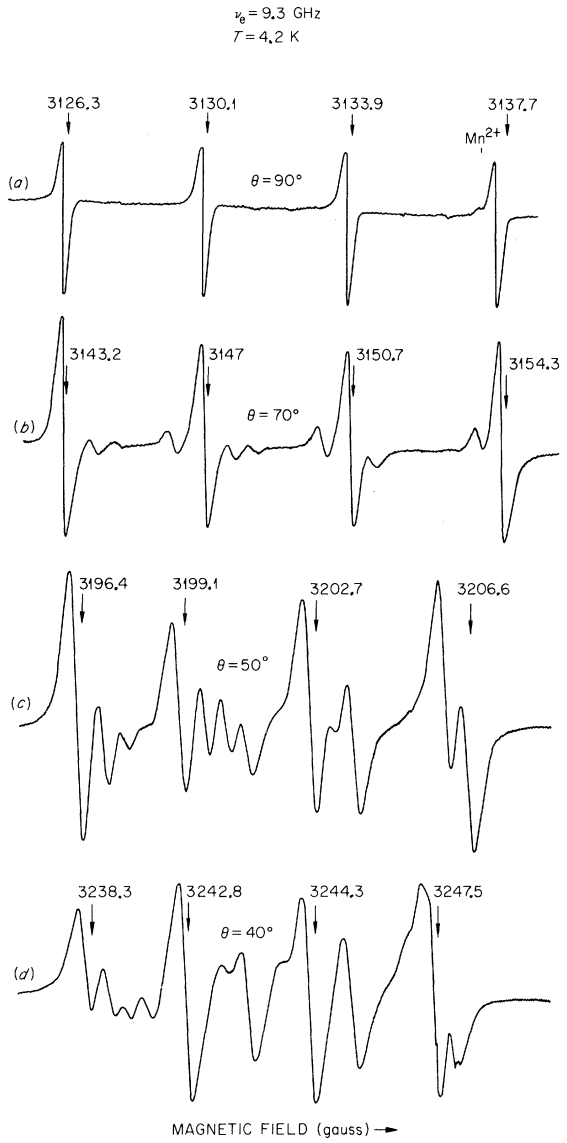

FIG. 2. EPR spectrum of the $[Na]^0$ center in CaO at various magnetic field orientations.

was observed with peak-to-peak width equal to the total hyperfine splitting at 4 K. Additional broadening of this line occurred up to 94 K, without any annealing of the centers being observed. The broadening of the spectral components in the range 54–94 K is suggestive of motional averaging of the hyperfine structure due to the trapped hole hopping between its six equivalent positons around the Na^+ ion. Above 94 K the lines were too broad to make accurate measurements.

Some features of the EPR spectrum of the $[Li]^0$ center were reported earlier by Schirmer.[9] This spectrum has certain characteristics which are similar to those of the $[Na]^0$ center. Thus the g tensor has cylindrical symmetry about a crystal ⟨100⟩ axis and the hyperfine structure due to ^7Li ($I = \frac{3}{2}$) is well resolved at some orientations. However, when the angle θ between $\vec{H}$ and the z axis of the defect is between 0° and 35°, the hyperfine structure collapses and, as shown in Fig. 3, a single line is observed. Moreover, the peak-to-peak separation in the derivative presentation of this single line is less at $\theta = 15°$ than at $\theta = 0°$. Hence it is concluded that $A_{\parallel}$ and $A_{\perp}$ are of opposite sign. An important characteristic of the hyperfine structure is the appearance of additional lines outside the main hyperfine lines at orientations between $\theta = 35°$ and 80°. Examples of this additional structure are shown in Fig. 3 for angles $\theta = 55°$, 45°, and 35°.

A detailed examination of the temperature de-

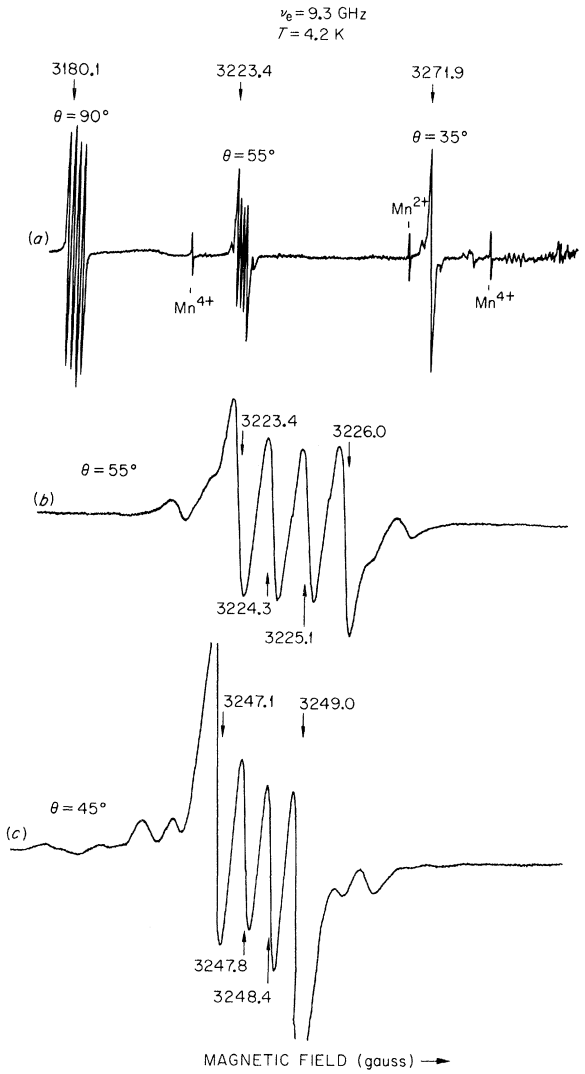

FIG. 3. EPR spectrum of the $[Li]^0$ center in CaO at various magnetic field orientations.

pendence of the $[Li]^0$ spectrum also revealed evidence of the trapped hole hopping around the Li^+ ion. The effects were observed for magnetic field orientations within the (100) plane, with $\theta = 45°$. First, we observed that the individual hyperfine components begin to broaden near 20–25 K. Second, the hyperfine structure for $\theta = 45°$ is motionally averaged to a single line near 77 K, whereas at $\theta = 90°$ hyperfine structure is averaged out near 105K. Finally, the difference $(g_\perp - g_\parallel)$ decreases with increasing temperature above 135 K, as shown in Fig. 4. Unfortunately, above 180 K the center decays thermally and an isotropic g value was never observed.

B. Spin-Hamiltonian Parameters

For both centers, the EPR results clearly require that $S = \frac{1}{2}$ and $I = \frac{3}{2}$. The hyperfine structure due to the 7% naturally abundant ^6Li could not be observed. The observed spectra were analyzed using the following spin Hamiltonian:

$$\mathcal{H} = \mu_B \vec{H} \cdot \overleftrightarrow{g} \cdot \vec{S} + \vec{I} \cdot \overleftrightarrow{A} \cdot \vec{S} + \vec{I} \cdot \overleftrightarrow{P} \cdot \vec{I} - g_N \mu_N \vec{H} \cdot \vec{I} , \tag{1}$$

where all symbols have their usual significance. In principle, the symmetry axes of the g, A, and P tensors may differ. However, the maximum and minimum hyperfine splittings occur at $\theta = 0°$ and $90°$, requiring that the g tensor and A tensor have the same symmetry axes. Furthermore, the accurate coincidence of the perpendicular components in a ⟨100⟩ crystal orientation implies that the quadrupole term is diagonal, and $P_x = P_y = 0$. The additional lines in Figs. 2 and 3 are due to the nominally forbidden $\Delta m_I = \pm 1$ and ± 2 transitions. These transitions lead to a quite complex hyperfine pattern in off-axis orientations, the line positions and intensities of which can only be predicted when both the quadrupole and nuclear g tensor are included in the spin Hamiltonian.

Approximate values for the parameters $g_\parallel, g_\perp, A_\parallel$, and $A_\perp$ were determined from the resonant fields in the $\theta = 0°$ and $90°$ orientations. The quadrupole term cannot be determined accurately from measurements in these two orientations. Consequently, the field positions of "allowed" and "forbidden" hyperfine transitions were measured at several orientations between $\theta = 0°$ and $90°$. Using the approximate parameters, tabulated values for g_N for Na and Li, [11] and themmeasured field positions as a starting point, the eigenvalue problem was solved by iterative procedures using a digital computer. The final spin-Hamiltonian parameters are:

$[Li]^0$

$$g_\parallel = 2.0019 \pm 0.0005 , \quad A_\parallel = \mp 0.006 \pm 0.05 \text{ MHz} ,$$

$$g_\perp = 2.0885 \pm 0.0005 , \quad A_\perp = \pm 3.87 \pm 0.02 \text{ MHz} ,$$

$$P \approx \mp 0.0027 \pm 0.05 \text{ MHz} ;$$

$[Na]^0$

$$g_\parallel = 2.0002 \pm 0.0005 , \quad A_\parallel = \pm 5.40 \pm 0.01 \text{ MHz} ,$$

$$g_\perp = 2.1234 \pm 0.0005 , \quad A_\perp = \pm 11.10 \pm 0.02 \text{ MHz} ,$$

$$P \approx \pm 1.2 \pm 0.2 \text{ MHz} .$$

The accuracy of these evaluations could be improved by use of the ENDOR technique.

C. Reorientation Effects

The temperature dependence of the $[Li]^0$ EPR spectrum was referred to briefly above. This may be considered in terms of the reorientational motion of the trapped hole around the Li^+ ion.[9] Such motion has no effect on the resonance spectrum until the reorientation time τ is of the order of the reciprocal linewidth. Lifetime broadening of the EPR line results. Increasing τ by increasing the temperature T leads to an averaging of the g tensor. Thus the high-temperature spectrum will consist of a single broad line, corresponding to the motionally averaged situation. For the $[Li]^0$ center there are two types of jumps which must be distinguished: (a) The hole may jump to any of the four equivalent O^{2-} ions situated in nearest-neighbor sites, or (b) the hole may invert across the Li^+ ion to the axially disposed O^{2-} ion. This latter type of motion seems less likely and is ignored for the purpose of this discussion.

The reorientation time of the motion as a function of temperature is easily obtained from the averaged-out spectrum. Since the reorientation motion is thermally activated, we can write

$$\frac{1}{\tau} = \frac{1}{\tau_0} e^{-E/kT} , \tag{2}$$

where E is the activation energy for the reorientation process. Under the conditions of the motionally averaged spectrum discussed above, $1/\tau$ is proportional to the broadened linewidth or the extent to which the g tensor is averaged out. Hence we can plot ΔH (Gauss) logarithmically as a function of T^{-1}, as shown in Fig. 5, and from the slope determine E. The experimental points are reasonably close to the straight line, obtaining $E = 0.04 \pm 0.01$ eV and $1/\tau_0 \sim 6 \times 10^8$ Hz.

D. Optical Spectra of V^-, $[Li]^0$, and $[Na]^0$ Centers in CaO

Figure 6 portrays the optical bands produced by irradiating different CaO crystals with ionizing radiation at 77 K. In "pure" CaO a weak band is observed at 1.85 eV which we attributed to V^- centers. This assignment is based upon the peak position, half-width (1.0 eV), thermal bleaching, and optical bleaching of the band relative to the V^- band in MgO.[12,13] In particular the V^- band is stable at

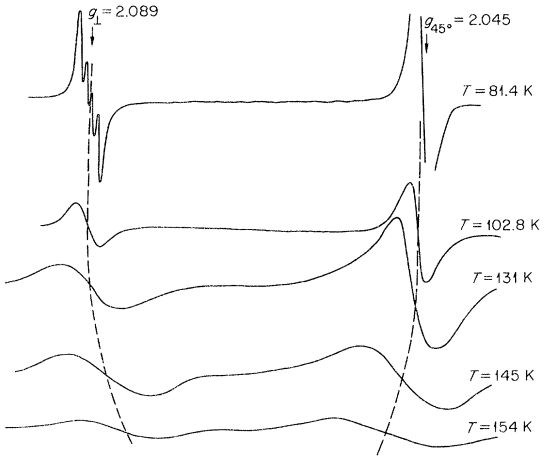

FIG. 4. Temperature dependence of the $[Li]^0$ EPR spectrum in CaO at 9.3 GHz.

4 K, unless exposed to light with λ near the band peak. Contrary to the situation in MgO, the V^- band in CaO is not particularly enhanced by quenching from high temperature prior to irradiation. In MgO the enhancement is attributed to the dissolution of $Mg(OH)_2$ precipitates at high temperature, leading to a high concentration of isolated OH^- ions in the MgO matrix.[14] Charge compensation for OH^- occurs by way of cation vacancies, which act as the trapping sites for the positive holes released by the irradiation. In MgO (Fig. 7), the changes in intensity of the composite (V^-, V_{OH}) band subsequent to annealing are shown. Our EPR studies show that after annealing and quenching from 1400 K, the relative concentrations of V^- and V_{OH} centers are in the ratio 1:2, whereas after long annealing at 800 K the concentrations are in the ratio 5:1. The slight shift in the band suggests that the V^- band occurs at 2.32 eV and the V_{OH} band at a little less than 2.19 eV. The infrared absorption of the present CaO crystals showed a conspicuously weak OH^- spectrum, so that the failure to enhance the V^- band by annealing prior to irradiation is not surprising. An accurate determination of the oscillator strength was not possible due to the uncertainty in the background of the optical band.

The most detailed optical/EPR correlations were made on the CaO:Li crystals. The intensity of the $[Li]^0$ EPR spectrum varied directly with the intensity of the optical absorption band at 1.73 eV. A demonstration of the thermal correlation is given in Fig. 8, which shows that the EPR and optical spectra anneal out together during the isochronal thermal treatments. Absorption bands due to other centers, such as Li pairs,[15] were neglected in analyzing the optical absorption due to the $[Li]^0$ centers. A slight discrepancy between the EPR and optical measurements, shown in Fig. 8, is due to our neglect of small background absorption bands which anneal out at different temperatures than the $[Li]^0$ band. The half-width of the 1.73-eV band is 1.0 eV. Using this value and Smakula's equation in Gaussian form, we find $f = 0.10 \pm 0.02$ for the oscillator strength of the $[Li]^0$ band. The $[Li]^0$ center annealing seems to be a one-stage process with the center becoming unstable at 195 K. A further demonstration of the optical/EPR correlation is apparent from the observation that, at 77 K, the EPR spectrum of the $[Li]^0$ center is readily bleached out by 1.7-eV photons.

For the CaO:Na crystals, an optical band at 1.52 eV (see Fig. 6) was observed which can be decomposed into two major bands, peaking at 1.39 and 1.64 eV. Correlation with EPR measurements showed that the former, which anneals at 165 K, is due to the $[Na]^0$ center. The defect responsible for the 1.64-eV band, which decays at 230 K, has not as yet been identified.

IV. DISCUSSION

Our results shall be discussed mainly in context with a model adopted by other authors.[9,13,16] The common feature of the V^-, $[Li]^0$, and $[Na]^0$ centers in alkaline-earth oxide crystals is the O^- ion which resides in sites with tetragonal symmetry (Fig. 1). For a free ion, the ground configuration of O^- is $(1s)^2(2s)^2(2p)^5$, corresponding to a ground-state ^2P term. When treated as a point imperfection in

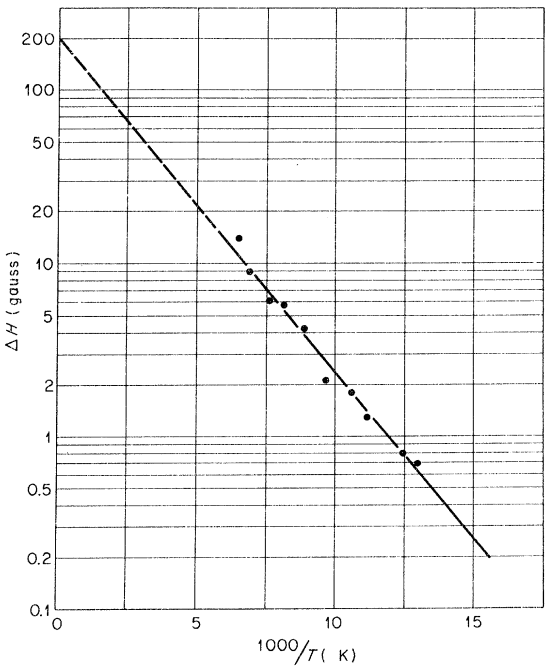

FIG. 5. Semilog plot of the $[Li]^0$ g shift vs reciprocal temperature. Here ΔH represents the shift $\Delta g = g_{\perp} - g_{45}$ with respect to Δg at $T = 1.5$ K.

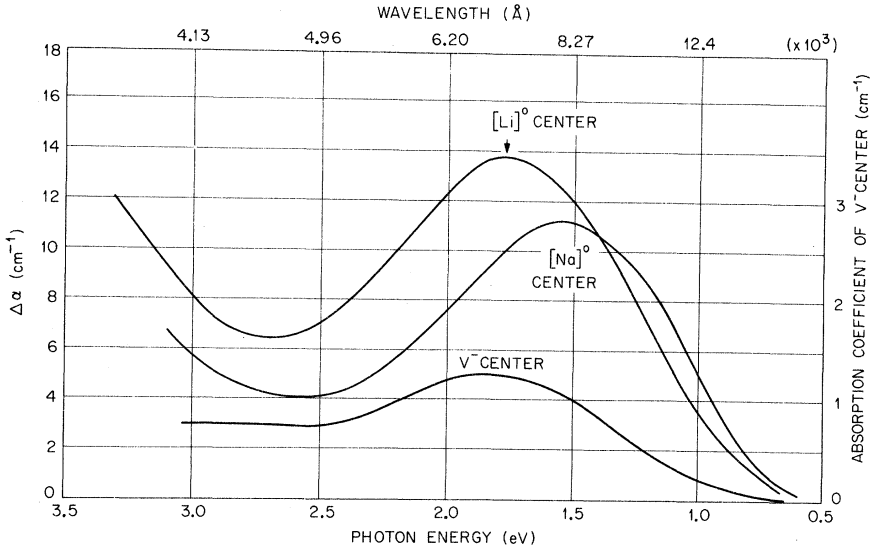

FIG. 6. Optical bands of trapped hole centers in CaO.

a lattice, the O^- ion experiences a crystal field potential which may be represented as the sum of contributions from the normal field of the lattice ions and the field due to the charge deficiency at the cation site. For free O^-, the first excited configuration, $2p^4 3s$, is ~60 000 cm^{-1} above the ground level, this energy being obtained by an extrapolation from the isoelectronic series O^- to Si^{5+} using Moore's tables.[17] Since this energy is already greater than the band gap of alkaline-earth-oxide crystals, only transitions within the ground configuration $2p^5$ will contribute to the optical absorption spectrum. Thus transitions can only occur between the levels which result from the splitting of the ^2P term into an orbital singlet $A(p_z)$ ground state and an orbital doublet $E(p_x, p_y)$ excited state by the tetragonal crystal field environment of the O^- ion (Fig. 9). The tetragonal crystal field is represented by the operator $\Delta[L_z^2 - \frac{1}{3}L(L+1)]$, which has energy eigenvalues of $-\frac{2}{3}\Delta$ and $\frac{1}{3}\Delta$, the orbital singlet state lying lowest. This corresponds to the hole occupying a p_z orbital pointing into the cation vacancy. The magnitude of Δ, the energy level splitting between the ground singlet A and excited doublet E states, is especially important in determining the g values of the center. Δ is determined primarily by the strength of the crystal field, which must include terms due to the distor-

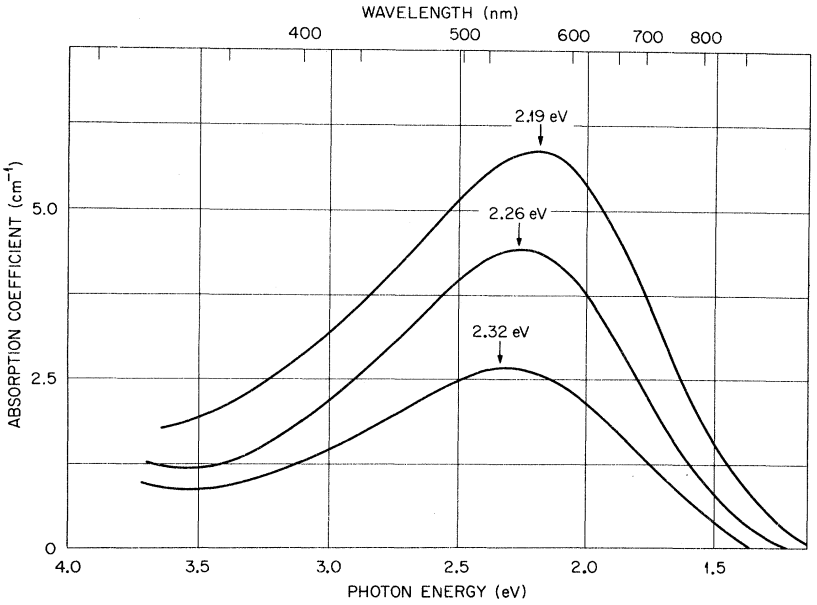

FIG. 7. Composite V^- and V_{OH} bands after ionizing irradiation in MgO. The spectra were for a crystal (a) "as grown," (b) after annealing and quenching from 1400 K, the ratio of V^- to V_{OH} centers being 1:2, (c) after long annealing (slow cooling) at 800 K, the ratio becoming 5:1.

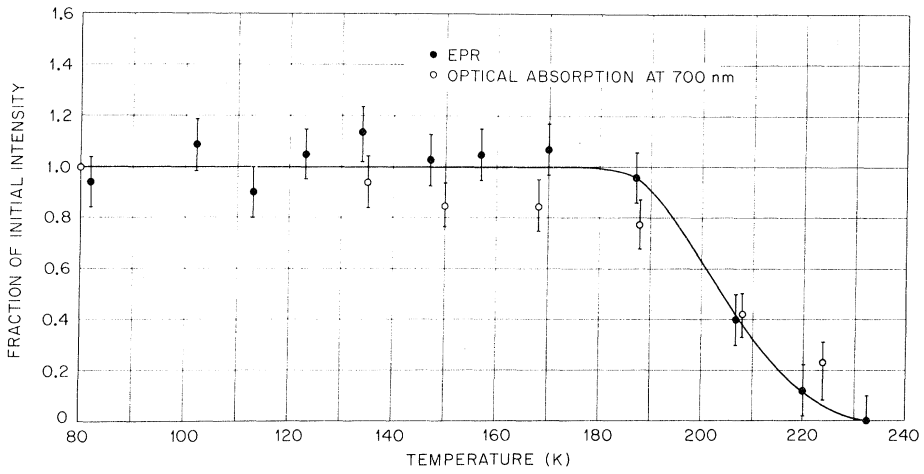

FIG. 8. Isochronal anneal of $[Li]^0$ in CaO.

tion of the lattice and configurational mixing with other levels.

There are several features of this model on which we should comment. First of all, since absorption of light induces essentially $p_z \rightarrow p_x$ or p_y excitations, only light polarized perpendicular to the defect axis can excite transitions. Second, these transitions involve no change in the orbital quantum number. Consequently, they are strongly forbidden by the Laporte selection rule and the oscillation strength should be quite small, of order 10^{-4}–10^{-5}. In MgO a broad band at 2.3 eV has been attributed to V^- centers. Failure to observe polarized bleaching in the V^- band below 20 K was interpreted as a consequence of the hole reorienting about the vacancy in a time short compared with the optical measuring time scale.[12,13]

In the presence of a magnetic field, the Hamiltonian appropriate to O^- is

$$\mathcal{H} = \Delta[L_z^2 - \tfrac{1}{3}L(L+1)] + \lambda[L_z S_z + \tfrac{1}{2}(L_+ S_- + L_- S_+)] + \mu_B \vec{H}\cdot(\vec{L} + 2\vec{S}), \quad (3)$$

where the first and third terms are the crystal field and Zeeman operators, respectively, and the second term describes the consequences of spin-orbit coupling. The effect of the spin-orbit operator is to admix the $p_x(-)$ and $p_y(-)$ excited wave functions with the $p_z(+)$ ground state, as depicted in Fig. 9. Similarly, $p_x(+)$ and $p_y(+)$ couple only to $p_z(-)$. The appropriate wave functions for the perturbed ground state are

$$\psi(\pm) = \mp\alpha p_x(\pm) - i\beta p_y(\mp) + \gamma p_z(\pm), \quad (4)$$

where the admixture coefficients α, β, and γ are given by

$$\alpha = \beta = -[\lambda/2(\Delta - \tfrac{1}{2}\lambda)]\gamma \quad (5)$$

and

$$\gamma = [1 + \lambda^2/2(\Delta - \tfrac{1}{2}\lambda)^2]^{-1/2}. \quad (6)$$

The g value may be calculated from the expectation value of the Zeeman interaction taken over the wave functions $\psi(\pm)$ given in Eq. (4). To second order in perturbation theory, the values of $g_\parallel$ and $g_\perp$ are given by[13,18]

$$g_\parallel = 2.00232[1 - \lambda^2/2(\Delta - \tfrac{1}{2}\lambda)^2] \quad (7)$$

and

$$g_\perp = 2.00232[1 - \lambda/(\Delta - \tfrac{1}{2}\lambda) - \lambda^2/2(\Delta - \tfrac{1}{2}\lambda)^2], \quad (8)$$

where λ is the spin-orbit coupling constant for the O^- ion. For a free O^- ion, $\lambda = -135\ cm^{-1}$, this value being obtained by extrapolation from the isoelectronic series, Si^{5+} to F^0.[17,19] Since λ is negative, Eq. (8) predicts that $g_\perp$ will be greater than the free electron g value. In a crystalline environment, λ will be modified by wave-function admixtures with states of the neighboring ions and the

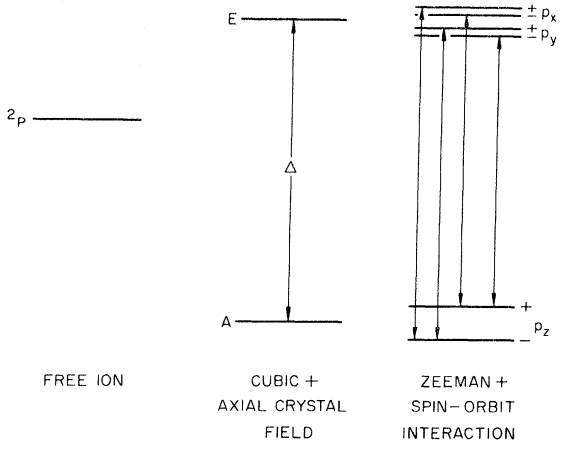

FIG. 9. Energy levels of O^- in axial crystal field.

TABLE I. Experimental and calculated parameters of trapped hole centers in CaO.

	Experiment		Calculated		
	$\Delta g_\perp$	$\Delta g_\parallel$	$\Delta(cm^{-1})$	$\lambda(cm^{-1})$	$\Delta g_\parallel$
V^-	$+67.9\times10^{-3}$	-1.2×10^{-3}	14900	−524	-1.2×10^{-3}
$[Li]^0$	$+86.2\times10^{-3}$	-0.4×10^{-3}	14000	−627	-1.9×10^{-3}
$[Na]^0$	$+121.1\times10^{-3}$	-2.1×10^{-3}	11200	−721	-3.7×10^{-3}

higher-lying states on the central ion.

Equations (7) and (8) relate the experimental g values to the effective spin-orbit coupling constant λ and transition energy Δ of the O^- ion in the crystal. A much simplified crystal field calculation[19] for $[Li]^0$ and $[Na]^0$ centers yields $\Delta = 3e^2\langle r^2\rangle/5R^3$, where e is the electronic charge, $\langle r^2\rangle$ is the radial integral of the O^- p functions, and R is the cation-anion separation. For V^- centers the result is $\Delta = 6e^2\langle r^2\rangle/5R^3$. The above expressions predict that the transition energy should be almost identical for the $[Li]^0$ and $[Na]^0$ centers, being one-half of the transition energy for the V^- center. Assuming that the optical absorption peaks correspond to Δ (Fig. 9), the experimental values of Δ for the V^-, $[Li]^0$, and $[Na]^0$ centers in CaO are compared in Table I. Clearly agreement is rather poor, suggesting that the simple electronic structure assumed for this center is inadequate in relation to the optical properties of these centers.

We have used the experimental values of Δ from the optical data to determine an effective spin-orbit coupling constant λ from the measured values of $g_\perp$ and Eq. (8). A particularly noticeable feature is that the magnitude of the spin-orbit parameters derived in this way are 4–5 times larger than the free ion value of $\lambda = -135\ cm^{-1}$. It is possible that sources of orbital momentum other than the central O^- ion are involved. The hyperfine structure clearly implicates the nearest-neighbor cations as possible contributors to the total spin-orbit parameter for the defect. In the present cases we have to consider overlap onto Li^+, Na^+, and Ca^{2+} ions: Effects due to Ca^{2+} are approximately constant for the three defects. Since in general the value of λ for a particular term increases with atomic number, it does seem reasonable that the spin-orbit coupling constant is larger for the $[Na]^0$ center than the $[Li]^0$ center. However, the increase by a factor 4–5 over the free ion λ is unexpectedly large, pointing to inadequacies in the assumed model. A possible source of error is that Δ overestimates the $p_z \rightarrow p_x$, p_y splitting. Further work on the nature of the excited states will be necessary to clear up this difficulty.

The values of $g_\parallel$ are also worthy of some interest since from Eqs. (7) and (8) it follows that $\Delta g_\parallel \approx -\frac{1}{4}(\Delta g_\perp)^2$. Values of $\Delta g_\parallel$ for the V^-, $[Li]^0$, and $[Na]^0$ centers calculated using this expression are also compared with the experimental shift in $g_\parallel$ in Table I. For the V^- center good agreement between the experimental and predicted value of $\Delta g_\parallel$ is observed. However, for the $[Li]^0$ and $[Na]^0$ centers, the predicted shifts in $g_\parallel$ are too large. Although the discrepancies are not dramatic relative to experimental inaccuracies, our g-value measurements seem to suggest that some other mechanism makes a positive contribution to $\Delta g_\parallel$. The hole is partially shared by six equivalent O^{2-} ions neighboring the cation deficiency. Assuming that the angular momentum on each oxygen ion can be summed separately, there is an isotropic positive g shift for the hole shared equally by the six O^{2-} ions, given by $\Delta g = -\frac{4}{3}\lambda/\Delta$.[20] Consequently, the tendency for the hole sharing will be reflected by a positive contribution to $\Delta g_\parallel$ given approximately by $-\frac{4}{3}(\lambda/\Delta)p$, where p is the probability of the hole being shared by the other equivalent O^{2-} ions. Thus the measured $\Delta g_\parallel$ in Table I imply that for the V^- center the probability p is negligibly small, whereas in the $[Li]^0$ and $[Na]^0$ centers it is larger.

V. HYPERFINE INTERACTION

We shall consider additional terms in the hyperfine interaction. The additional terms are cross terms due to (i) electron-orbital interaction with the impurity nucleus[21] and (ii) electronic dipole interaction with the nuclear dipoles, in combination with spin-orbit interaction.[22] Schirmer[9] has shown that (ii) is negligible for the hole centers discussed here. The correction due to spin-orbit mixing of the excited $E(p_x, p_y)$ state with the $A(p_z)$ state is given by[21]

$$\mathcal{H}(IS) \approx (2\lambda/\Delta)(\tfrac{1}{2}b)(I_xS_x + I_yS_y)\ . \tag{9}$$

Hence,

$$A_\parallel = a + 2b,\quad A_\perp = a - b(1 + \tfrac{1}{2}\Delta g_\perp)\ . \tag{10}$$

Using Eq. (10) and the $A_\parallel$ and $A_\perp$ values quoted earlier, we find

$[Li]^0$ $\quad a = \pm 2.52$ MHz, $\quad b = \mp 1.26$ MHz;

$[Na]^0$ $\quad a = \pm 9.14$ MHz, $\quad b = \mp 1.84$ MHz .

The parameters a and b are of opposite sign: Their absolute signs are experimentally indeterminate. Since a and b contain the product $\mu_B\mu_N$, this behavior is clearly anomalous. For other trapped hole centers, V_{OH}, V_F, etc., no such hyperfine anomaly is observed and the magnitude of b is given to within ~3% by the electron-nuclear dipolar interaction of conventional form.[4] It seems reasonable to assume that such is the case also for the $[Li]^0$ and $[Na]^0$ centers, with b positive and the Fermi contact term a negative. Since

$$a = \tfrac{8}{3}\pi\mu_B\mu_N(|\psi(0)\uparrow|^2 - |\psi(0)\downarrow|^2)\ , \tag{11}$$

such a conclusion implies that some unknown mech-

anism transfers more ↓ spin than ↑ spin to the Na and Li nuclei. Orthogonalization of the simple O^- $2p_z$ function to the occupied core orbitals on the alkali ions results in a positive value for the contact term, nor can exchange polarization explain the apparent negative sign for a.[9] As previously suggested, the discrepancy may arise from the assumption that a pure p_z state on the O^- ion is involved. The axial electric field acting upon the O^- ion admixes the excited $|3s\rangle$ state of the O^- ion into the ground $|p_z\rangle$ state. Such wave-function admixture influences the hyperfine structure parameters and the optical properties of these defects. As discussed earlier, pure $p_z \rightarrow p_x$, p_y transitions should be exceedingly weak. However, the possible presence of s-p admixtures in the ground state, which enhance the oscillator strength of the $A \rightarrow E$ optical transitions, is indicated by the measured values of the oscillator strength, typically ≈ 0.1. Calculations involving s-p hybridization which include also admixtures from neighboring ions are currently in progress.[23] The anisotropic hyperfine constants b for both centers are consistent with a mainly dipolar form for the electron-nuclear interaction.

VI. CONCLUDING REMARKS

The optical and EPR results on the $[Na]^0$ and $[Li]^0$ trapped hole centers presented here seem to imply that the model of a hole trapped in a pure p_z state of the O^- ion is inadequate to explain the known properties of these centers. The large half-width and oscillator strength of the optical transitions and the extemely large values of λ required to account for the observed EPR g shifts constitute a serious challenge to this model. If we assume that the λ values of the O^- ions do not differ appreciably from the free ion value, the value of Δ is correspondingly smaller. The lack of observable bands at such low energies need not be disturbing since these transitions are expected to be forbidden. However, we must then explain the origin of the observed optical bands that are correlated with the EPR spectra.

†Research sponsored by the U. S. Atomic Energy Commission under contract with Union Carbide Corporation.

*Permanent address: University of Alabama, Birmingham, Ala.

‡Permanent address: Keele University, Staffordshire, England.

[1]J. E. Wertz, P. Auzins, J. H. E. Griffiths, and J. W. Orton, Discussions Faraday Soc. 28, 136 (1959).

[2]The system of nomenclature used here is that suggested by E. Sonder and W. A. Sibley, *Defects in Crystalline Solids*, edited by J. H. Crawford, Jr. and L. M. Slifkin (Plenum, New York, 1971).

[3]G. Rius and R. Cox, Phys. Letters 27A, 76 (1968).

[4]See, for example, P. Kirklin, P. Auzins, and J. E. Wertz, J. Phys. Chem. Solids 26, 1067 (1965); W. C. O'Mara, J. J. Davies, and J. E. Wertz, Phys. Rev. 179, 816 (1969); B. Henderson, J. L. Kolopus, and W. P. Unruh, J. Chem. Phys. 55, 3519 (1971).

[5]W. C. O'Mara, Ph. D. thesis (University of Minnesota, 1969) (unpublished); L. Halliburton, D. L. Cowan, and L. V. Holroyd, Bull. Am. Phys. Soc. 15, 760 (1971).

[6]A. J. Shuskus, J. Chem. Phys. 39, 849 (1963).

[7]J. W. Culvahouse, L. V. Holroyd, and J. L. Kolopus, Phys. Rev. 140, 1181 (1965).

[8]J. T. Suss, Ph. D. thesis (Hebrew University, Jerusalem, 1966) (unpublished).

[9]O. F. Schirmer, J. Phys. Chem. Solids 32, 499 (1971).

[10]M. M. Abraham, C. T. Butler, and Y. Chen, J. Chem. Phys. 55, 3752 (1971).

[11]G. Seidel and H. C. Wolf, *Physics in Colour Centres*, edited by B. Fowler (Academic, New York, 1971).

[12]J. E. Wertz, G. S. Saville, P. Auzins, and J. W. Orton, J. Phys. Soc. Japan, Suppl. II 18, 305 (1963); Y. Chen and W. A. Sibley, Phys. Rev. 154, 842 (1967).

[13]A. E. Hughes and B. Henderson, in Ref. 2.

[14]B. Henderson and W. A. Sibley, J. Chem. Phys. 55, 1276 (1971).

[15]H. T. Tohver and B. Henderson (unpublished).

[16]W. E. Hagston, J. Phys. C 3, 1233 (1970).

[17]C. E. Moore, Natl. Bur. Std. (U. S.) Circ. 467 (1969).

[18]J. R. Brailsford, J. R. Morton, and L. E. Vannotti, J. Chem. Phys. 49, 2237 (1968).

[19]R. Bartram, C. E. Swenberg, and J. T. Fournier, Phys. Rev. 139, A941 (1965).

[20]T. C. Ensign and S. E. Stokowski, Phys. Rev. B 1, 2799 (1970).

[21]D. Shoemaker, Phys. Rev. 149, 693 (1966).

[22]A. N. Jette, Phys. Rev. 184, 604 (1969).

[23]R. F. Wood (private communication).